Effect of dendritic orientation on the high temperature oxidation kinetic of tantalum-containing nickel-base alloys

P. Berthod · C. Vébert · L. Aranda

Abstract The aim of this work is the study of the possible effect of surface dendritic orientation on the high-temperature oxidation behavior of two chromia-forming Ni-base alloys with two tantalum contents ($3\%_{wt}$ and $6\%_{wt}$). Samples were prepared by special cutting orientation with regard to the external surface. Thermogravimetry tests were run at 1,000 °C, 1,100 °C and 1,200 °C and parabolic oxidation constants were determined taking into account the effect of the transient oxidation. When the sample surface is mainly parallel to the dendritic network, the oxidation parabolic constant can be higher than for a surface perpendicular to dendrites. It occurs only for temperatures that depend on the alloy. Inversely, the transient oxidation linear constant is generally higher for the perpendicular orientation than for the parallel one.

Introduction

When obtained by a classical foundry way, the microstructure of metallic alloys depends on their chemical composition but also on the solidification conditions. For example, the thermal gradient existing during the solidification governs the general direction of crystals growth, then dendrites and grain boundaries orienta-

P. Berthod (✉) · C. Vébert · L. Aranda
Laboratoire de Chimie du Solide Minéral (UMR 7555), Faculté des Sciences et Techniques, Université Henri Poincaré Nancy 1, BP 239, 54506 Vandoeuvre-Les-Nancy Cedex, France
e-mail: patrice.berthod@lcsm.uhp-nancy.fr

tions. The latter are generally considered as special diffusion paths for species involved in the oxidation mechanisms [1]. Then it can be thought that the kinetics of high-temperature oxidation of superalloys could locally depend on dendrites orientation, like it was previously seen for different complex Co-base and Ni-base cast superalloys [2]. This possible effect was studied here at different high temperatures in the case of two chromia-forming Ni-base cast alloys which also contain tantalum.

Effect of the thermal gradient on the dendrite orientation

A microstructural evolution usually exists in alloys obtained by a classical foundry way, from the external surface towards the last point to solidify [3–5]. Near the mold wall (Fig. 1), among the first numerous very small crystals that appeared here, only a little number of them pursue their growth in the next zone. These ones are favorably oriented with regard to the local thermal gradient, which is often perpendicular to the mold wall. Thus, after a skin zone containing very small and randomly oriented grains, a columnar zone develops with an oriented microstructure. Here dendrites are mainly perpendicular to the mold wall. The third zone, where solidification finished, contains coarser dendrites that are randomly oriented again, because of the absence of any very marked gradient. After machining, a cast piece may present locally external surfaces with different grain sizes and also different dendrites orientations. Even if dendrites are not all either parallel or perpendicular to the external surface, like it could be encountered for directionally solidified (DS) alloys, a

Fig. 1 The three different microstructure zones which can be met from the mold wall in a metallic piece obtained by a classical foundry way

cortical zone (very fine grains)

columnar zone (dendrites mainly perpendicular to the mold)

equiaxed zone (coarse and randomly oriented dendrites)
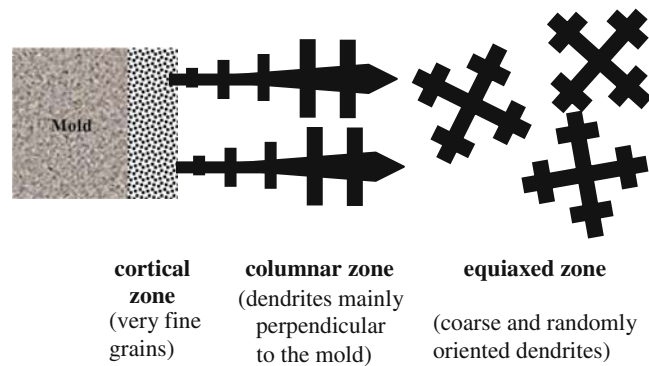
global effect on the local oxidation kinetic may exist. The latter will be better studied with specially machined equiaxed alloys than with DS alloys the microstructure of which is too specific.

Materials and methods

Synthesis of the alloys

Two Ni-base alloys were elaborated using a high frequency induction furnace under argon gas, and solidified in a water-cooled copper crucible (cone-shaped ingots of about 100 g and height = maximal diameter = 30 mm). They were synthesized from pure elements (more than 99.9%): Ni (supplier: Eramet), Cr (supplier: Alfa Aesar), Ta (supplier: Aerometal) and C (graphite). The obtained chemical compositions are given in Table 1.

High temperature oxidation tests and mathematical processing

Samples were parallelepipeds of approximately 10 mm × 10 mm × 2 mm. Cutting orientation was chosen in order to obtain square faces that are either parallel or perpendicular to dendrites (Fig. 2). For each sample, the total mass gain is the sum of two contributions which can be uncoupled. The oxidation rates of the parallel surface $S_{//}$ and of the perpendicular surface $S_\perp$ exist together in the global mass gain rate (Eq. 1). Then, the two parabolic constants $Kp_{//}$ and
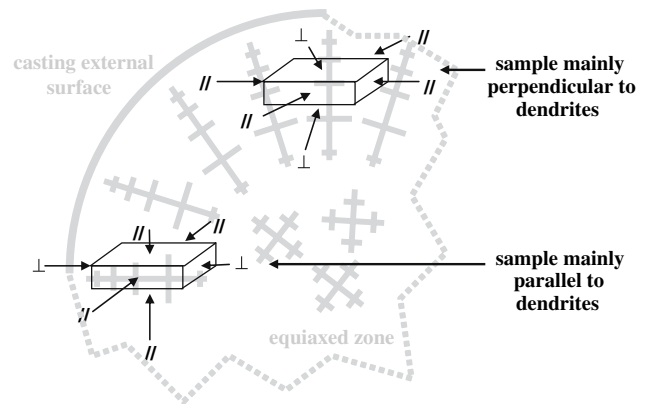
Fig. 2 Cutting modes for samples mainly parallel or mainly perpendicular to dendrites

$Kp_\perp$, that describe the two local oxidation rates, appear as the two unknown values of a linear equation (Eq. 2), in which they are related to the measured global constant Kp. For a same alloy and a same temperature, solving the two linear equations (Eq. 2) written for the two types of samples gives both $Kp_{//}$ and $Kp_\perp$.

$$\frac{\Delta m}{S}(t) = \frac{\Delta m_{//}(t) + \Delta m_\perp(t)}{S_{//} + S_\perp} = \frac{S_{//}}{S_{//} + S_\perp}\sqrt{2\,Kp_{//}}\,\sqrt{t} \\ + \frac{S_\perp}{S_{//} + S_\perp}\sqrt{2\,Kp_\perp}\,\sqrt{t} \tag{1}$$

$$\frac{S_{//}}{S}\sqrt{2\,Kp_{//}} + \frac{S_\perp}{S}\sqrt{2\,Kp_\perp} = \sqrt{2\,Kp} \tag{2}$$

Oxidation runs were performed using a Setaram TGA92 thermobalance. Alloys were exposed at 1,000 °C, 1,100 °C and 1,200 °C for 100 h to a flow of synthetic air (80%N$_2$–20%O$_2$) of about 1.5 l/min. The heating rate and the cooling rate down to room temperature were 20 °C/min and 10 °C/min, respectively. The mass gain was recorded every 74 s.

Table 1 Chemical compositions of the two studied alloys

Alloys	Weight contents (%)			
	Ni	Cr	C	Ta
H alloy	Bal.	30	0.40	5.4
L alloy	Bal.	30	0.20	2.0

All the obtained mass gain curves showed an initial linear part (of the (Eq. 3) type) followed by a parabolic part (of the (Eq. 5) type) by which it was possible to determine a parabolic Kp constant.

$$\frac{\Delta m}{S} = K_l\, t \tag{3}$$

$$K_l = K_{l_o}\, e^{\frac{-Q}{RT}} \tag{4}$$

$$\frac{\Delta m}{S} = \sqrt{2\,Kp}\,\sqrt{t} \tag{5}$$

The oxide thickness obtained before the beginning of the parabolic oxidation must be taken into account for the determination of Kp. Then, to process the obtained file we used the same procedure which we apply in a previous work [6] and which can be resumed as it follows. Oxidation during heating and the linear isothermal oxidation each induced a first mass gain before parabolic oxidation took place. The initial mass gain is the sum (Eq. 6) of a heating part (first term) and of a linear isothermal part (second term):

$$\frac{\Delta m_o}{S} = K_{l_o} \int_{273\,K}^{T_{test}} e^{\frac{-Q}{RT(t)}}\, dt + \left(\frac{\Delta m}{S}\right)_L \approx K_{l_o}$$

$$\left(\sum_{n=1}^{N} e^{\frac{-Q}{R\left(273\,K + R_H\, n\,\Delta t\right)}}\right) \Delta t + \left(\frac{\Delta m}{S}\right)_L \tag{6}$$

where:

– K_{l_o} and Q, the Arrhenius constants of the linear constant K_l (Eq. 4), were deduced from the K_l values obtained for 1,273 K, 1,373 K and 1,473 K
– R_H is the heating rate,
– Δt is the recording time increment (74 s),
– N is the number of recording paths during the heating $(N = (T_{test} - 273\,K)/(R_H\,\Delta t))$, and $(\Delta m/S)_L$ is the mass gain during the isothermal linear oxidation.

When the external oxide scale becomes continuous, the Wagner's differential equation describes the parabolic mass gain kinetic $\Delta m_P/S$ (Eq. 7). Its integration leads to (Eq. 8).

$$\frac{d(\Delta m_P/S)}{dt} = \frac{Kp}{(\Delta m_p/S + \Delta m_o/S)} \tag{7}$$

$$Kp = \frac{1}{2\,(t - t_o)} \left[(\Delta m_p/S + \Delta m_o/S)^2 - (\Delta m_o/S)^2\right] \tag{8}$$

Knowing the values of $\Delta m_o/S$ and of t_o (instant at which the parabolic oxidation took place) the value of

Kp can be obtained without any error caused by the mass gain obtained before.

For 1,100 °C and 1,200 °C, the volatilization of the external Cr_2O_3 scale (partly oxidized into gaseous CrO_3) was taken into account by adding the Kv t quantity (Eq. 9), in order to get a value closer to the real Kp constant.

$$Kp = \frac{1}{2\,(t - t_o)} \left[((\Delta m_p/S + Kv\,t) + \Delta m_o/S)^2 - (\Delta m_o/S)^2\right] \tag{9}$$

The volatilization constant Kv is the rate of mass loss per surface unit area due to the volatilization of re-oxidized chromia. The values of Kv for 1,100 °C and 1,200 °C used here were the ones that were directly determined in a previous work [7] for similar alloys:

Kv = 2.4×10^{-10} g cm^{-2} s^{-1} (1,100 °C) and 46×10^{-10} g cm^{-2} s^{-1} (1,200 °C).

To finish, on the time range where oxidation is linear on both the part parallel to dendrites and the perpendicular one, the global K_l is a linear combination of two contributions (Eq. 10), like for the parabolic constants. The uncoupling (Eq. 10) leads to the $K_{l//}$ and $K_{l\perp}$ constants.

$$\frac{S_{//}}{S}\, K_{l//} + \frac{S_\perp}{S}\, K_{l\perp} = K_l \tag{10}$$

Examination of the oxidized samples

After testing, the surface of the oxidized samples became electrically conductive by a gold layer deposited by cathodic plasma pulverization. Then the external chromia layer was mechanically protected by a sufficiently thick electrolytic nickel coating. Thereafter samples were cut, embedded in resin, polished and examined using a Philips XL30 Scanning Electron Microscope (SEM), under a 20 kV acceleration voltage. Spot analysis and concentrations profiles were performed using Energy Dispersive Spectroscopy (EDS) coupled with the SEM. Identification of phases like carbides and oxides and Cr and Ta contents profiles were performed with a Cameca SX100 WDS microprobe.

Results

Initial microstructures of the alloys

The bulk microstructures of the as-cast alloys are illustrated by the SEM photographs presented in

Fig. 3. The two alloys own first an austenitic matrix which solidified with the form of dendrites. They also contain two types of carbides in the grain boundaries. Chromium carbides and tantalum carbides precipitated at the end of solidification forming an eutectic with matrix, with the Cr_7C_3 and TaC stoichiometries. These carbides are known to be very useful for strengthening at high temperatures [8, 9]. Carbides are obviously more present in the high carbon alloy (H alloy) than in the low carbon one (L alloy).

Oxidation rates

Oxidation runs were performed on the two alloys for the two main dendrites orientations and for the three temperatures 1,000 °C, 1,100 °C and 1,200 °C. All curves started by a linear isothermal part (transient oxidation) before the parabolic oxidation began. The latter led thereafter to a more or less long parabolic part of curve. Indeed, detachments of the external and continuous oxide scale often occurred and induced jumps of the mass gain. Some of thermogravimetry tests were started again but detachments occurred again. Thus, half of the presented curves are still
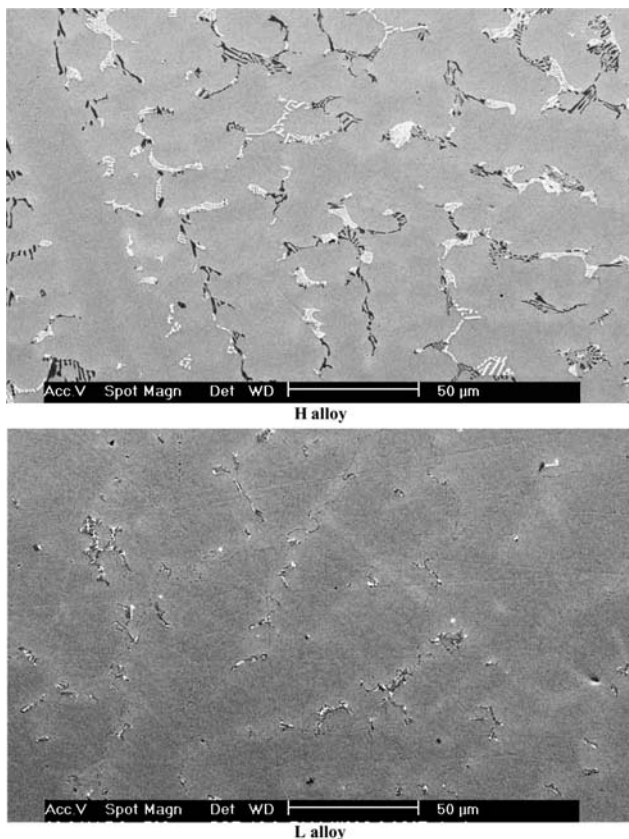
Fig. 3 As-cast microstructures of the two alloys

affected by one (or several) external oxide detachment. Fortunately the parabolic part was always sufficiently long (about 50 h) to allow the determination of the parabolic constants. Figure 4 shows the part of the obtained curves that follows the isothermal linear oxidation, after addition of the Kv t linear term to correct from the mass loss by chromia volatilization for 1,100 °C and 1,200 °C. The two mass gain curves corresponding to a same alloy and a same temperature but for the two orientations were plotted together in a same graph.

In most cases there is no real difference for the oxidation rate between the two orientations, since the two curves are almost superimposed, at least for the first parabolic part before the jump when it exists. However, two cases are different from the others: L alloy at 1,200 °C and H alloy at 1,000 °C. Indeed, in these cases, the curve corresponding to the parallel orientation is sensibly above the one corresponding to the perpendicular orientation.

Thereafter it was mathematically proceeded as previously explained. Table 2 shows the values of K_1 obtained for all the oxidation tests and the calculated $\Delta m_o/S$ mass gains that already existed before the parabolic oxidation. For each sample, i.e. each alloy and each main orientation, the linear constant logically increases with temperature and effectively follows an Arrhenius law (see example in Fig. 5). The activation energies presented in the last column are those which were employed to estimate the initial mass gains by oxidation during heating before test. One also can see that the linear constants seem to be higher for H alloy than for L alloy (except for 1,000 °C), and when the external surface is mainly perpendicular to dendrites than for the parallel orientation (at all temperatures). The same observations can be done for the mass gains before parabolic oxidation. This tendency is enhanced after uncoupling as shown in Table 3 in which it clearly appears that the orientation has directly an influence of the linear oxidation rate, especially for 1,200 °C.

After having exploited the values of the global linear constants, the global parabolic constants were obtained and they are given in Table 4. The parabolic constants also increase with temperature and are often different for the two orientations. However, the relative differences are the highest for H alloy at 1,000 °C (+31% for the parallel orientation) and for L alloy at 1,200 °C (+44% for the parallel orientation). This tends to confirm what it was seen about the raw mass gain curves. Like for the linear constants, the uncoupling enhances the differences (Table 5): the real differences existing between the two types of orientation as well as the differences due to the usual little
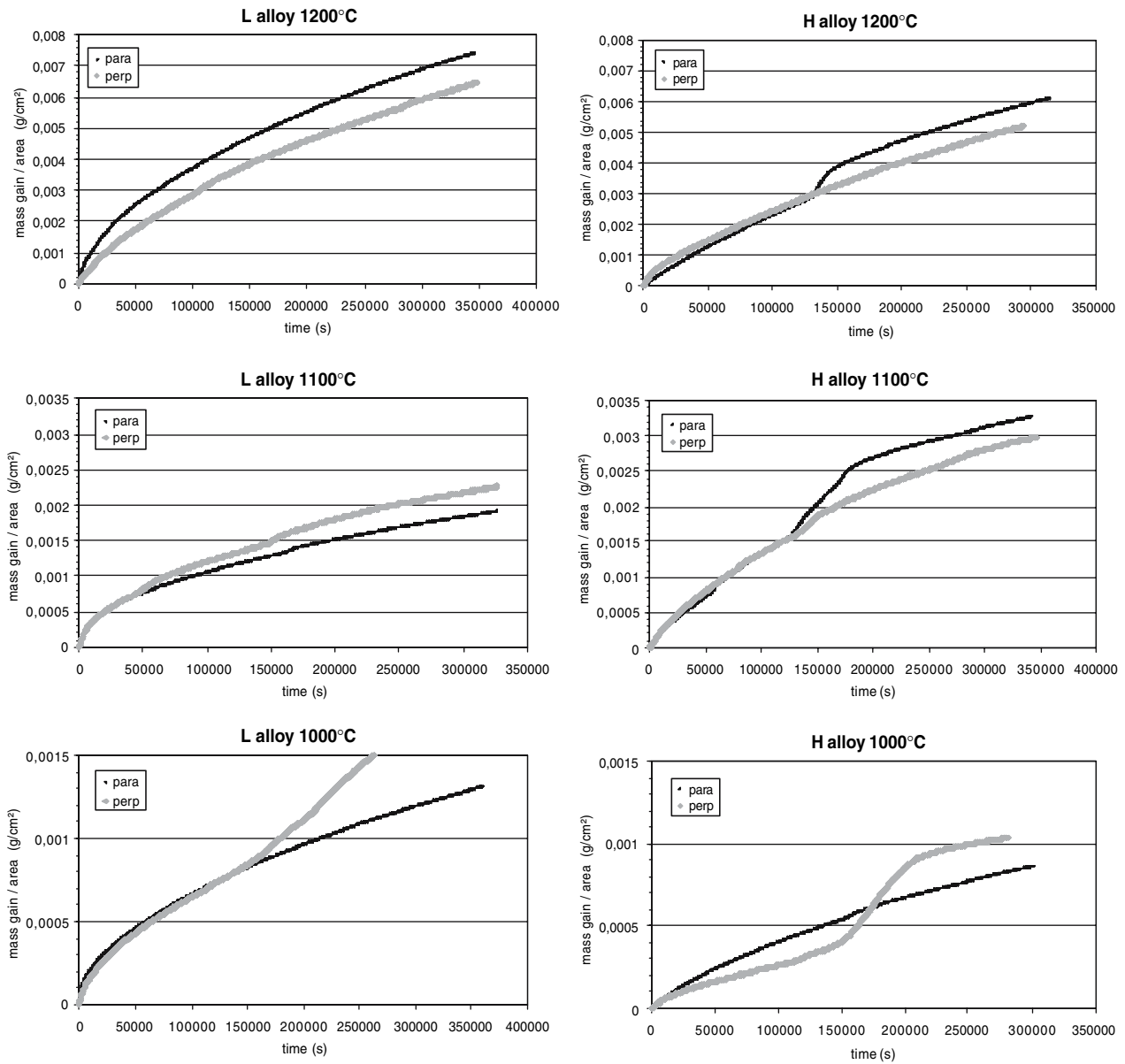
Fig. 4 Mass gain curves for the two orientations plotted on a same graph for a given alloy and a given temperature (first linear parts were removed from all curves here)

Table 2 Global oxidation linear K_l constants (10^{-8} g cm^{-2} s^{-1}) and values of the calculated $\Delta m_o/S$ mass gains already existing before the parabolic oxidation (in mg/cm^2)

Alloy	Temperature (°C)			Activation energy (kJ mol^{-1})
	1,000	1,100	1,200	
H alloy				
//	1.12 (0.651 mg/cm^2)	8.84 (1.25 mg/cm^2)	33.3 (4.82 mg/cm^2)	265
⊥	1.29 (1.06 mg/cm^2)	11.8 (1.32 mg/cm^2)	41.7 (5.52 mg/cm^2)	272
L alloy				
//	2.65 (0.113 mg/cm^2)	3.58 (2.08 mg/cm^2)	14.2 (4.18 mg/cm^2)	129
⊥	2.63 (0.096 mg/cm^2)	4.13 (2.52 mg/cm^2)	20.6 (4.59 mg/cm^2)	158
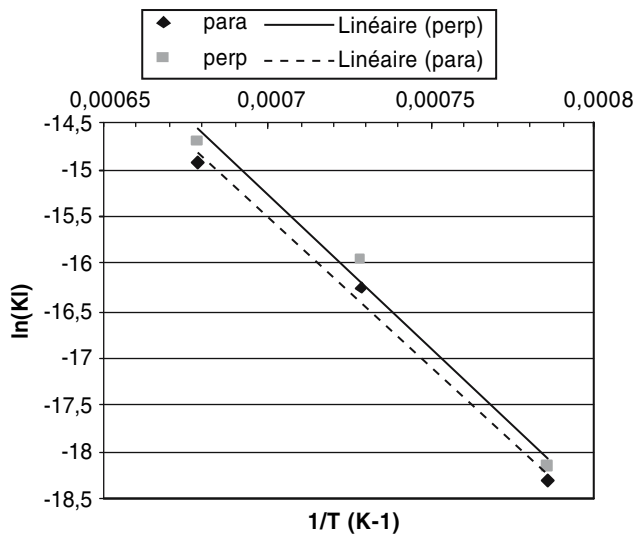
Fig. 5 Variation with temperature of the global K_1 values (expressed in $g\,cm^{-2}\,s^{-1}$) plotted in an Arrhenius graph (here for H alloy and the two orientations)

lack of reproducibility of thermogravimetry tests. Thus one must be careful for the interpretation of the calculated differences. It is the reason why one considered only the more marked differences that are too evident and cannot result from a problem of reproducibility. In this way, the $Kp_{//}$ is equal to three times $Kp_{\perp}$ for H alloy at 1,000 °C and two times for L alloy at 1,200 °C. The parabolic constant of each type

Table 3 Uncoupled oxidation linear constants (10^{-8} g cm^{-2} s^{-1})

Alloy	Temperature (°C)			Activation energy (kJ mol^{-1})
	1,000	1,100	1,200	
H alloy				
$K_{1//}$	1.02	8.20	27.2	257
$K_{1\perp}$	1.60	13.4	48.4	267
L alloy				
$K_{1//}$	2.65	3.14	11.7	113
$K_{1\perp}$	2.63	4.53	23.5	169

Table 4 Global oxidation parabolic Kp constants (10^{-12} g^2 cm^{-4} s^{-1})

Alloy	Temperature (°C)		
	1,000	1,100	1,200
H alloy			
//	3.24	24.9	137
⊥	2.48	24.8	126
L alloy			
//	2.46	13.3	117
⊥	2.21	16.1	81.5

Table 5 Uncoupled oxidation parabolic constants (10^{-12} g^2 cm^{-4} s^{-1})

Alloy	Temperature (°C)			Activation energy (kJ mol^{-1})
	1,000	1,100	1,200	
H alloy				
$Kp_{//}$	3.72	24.9	145	285
$Kp_{\perp}$	1.36	24.7	117	349[a]
L alloy				
$Kp_{//}$	2.49	11.2	133	308
$Kp_{\perp}$	2.15	18.2	67.5	270

[a] The three points are not really aligned

of surface more or less follows an Arrhenius law (example of Fig. 6), the activation energies of which are given in the last column of Table 5.

It can be also noted that it could sometimes exist an apparent bad agreement between the order of Kp constants and the order of mass gain curves, for the two alloys at a same temperature (particularly 1,000 °C and 1,200 °C). It only results from the difference of transient oxidation duration, then the difference of mass gain before the beginning of parabolic oxidation (which is taken into account for the Kp determination) and of the curve part where the parabolic constant was measured.

Observation of the oxidation front

After oxidation tests all samples were metallographically prepared and examined using a Scanning Electron Microscope. Unfortunately, the chromia layer had always totally quitted the surface of the samples, then it was not possible to analyze it. However, it was
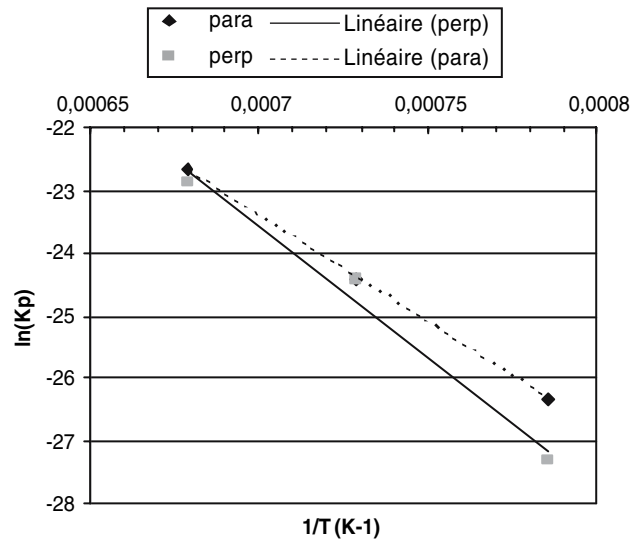
Fig. 6 Variation with temperature of the uncoupled $Kp_{//}$ and $Kp_{\perp}$ values (expressed in g^2 cm^{-4} s^{-1}) plotted in an Arrhenius graph (here for H alloy and the two orientations)

possible to examine the sub-surface deterioration of the alloy by oxidation (Fig. 7).

From the external surface, all samples exhibit a first zone that lost its initial carbides. For each alloy the depth of this carbide-free zone increases with temperature. Its depth also seems to be higher for the L alloy than for the H alloy, the carbide network of which is denser (Fig. 8).

On a thin outer part this zone also contains internal oxides, which were identified as being $CrTaO_4$ by WDS microanalysis. These oxides seem to be more present for the H alloy than for the L alloy which contains less tantalum. These oxides almost form a continuous layer along the external surface of the H alloy. Between the carbide-free zone and the bulk there is often an intermediate zone in which carbides are different compared to the ones still present in the bulk: darker, coarser or having precipitated in the matrix. These phenomena were explained in previous works [10–12] in the case of others alloys also reinforced by carbides: they result from an inwards diffusion of carbon atoms released by the dissolving carbides.

Concerning the dendritic orientation, one does not see real differences about both the carbide-free zone and the internal oxides, between the main faces of the two types of samples for a same alloy and a same temperature.

WDS profiles

The evolution of contents of both chromium and tantalum were analyzed from the external surface towards the bulk until the values remain constant. Two profiles were performed by sample and the results that are presented respectively in Tables 6 and 7 are the obtained average values.

The chromium profiles show two successive gradients for all samples at 1,000 °C and 1,100 °C. The first one corresponds to the carbide-free zone for 1,000 °C and 1,100 °C, while the second one exists deeper in the bulk where carbides are still here. However, the second Cr gradient is almost negligible for 1,200 °C and it can be considered that it does not exist (Fig. 9). For all alloys, when the temperature increases, the depths of the two Cr gradients also increase while the modulus of the gradient decrease. Between the alloys the Cr gradients are higher and their depths are smaller for the L alloy than for the H alloy at 1,000 °C while these tendencies disappear for the two highest temperatures. Between the two orientations, some differences can be

Fig. 7 Surface microstructural state of all L-alloy samples after oxidation test
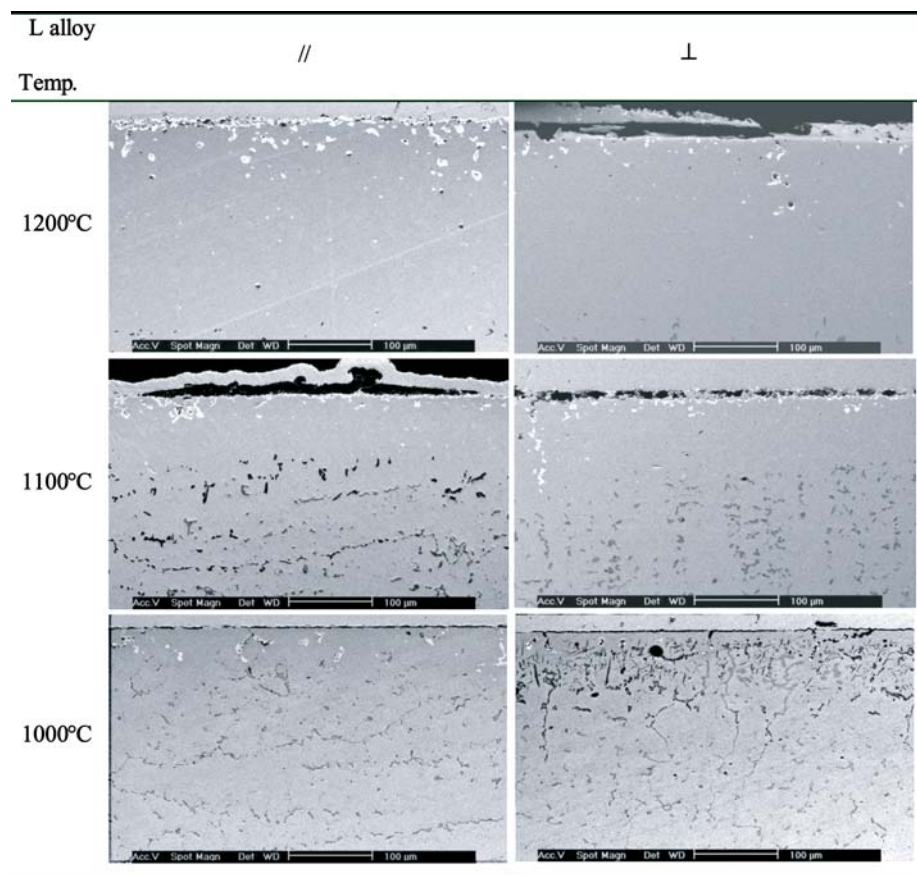
Fig. 8 Surface microstructural state of all H-alloy samples after oxidation test
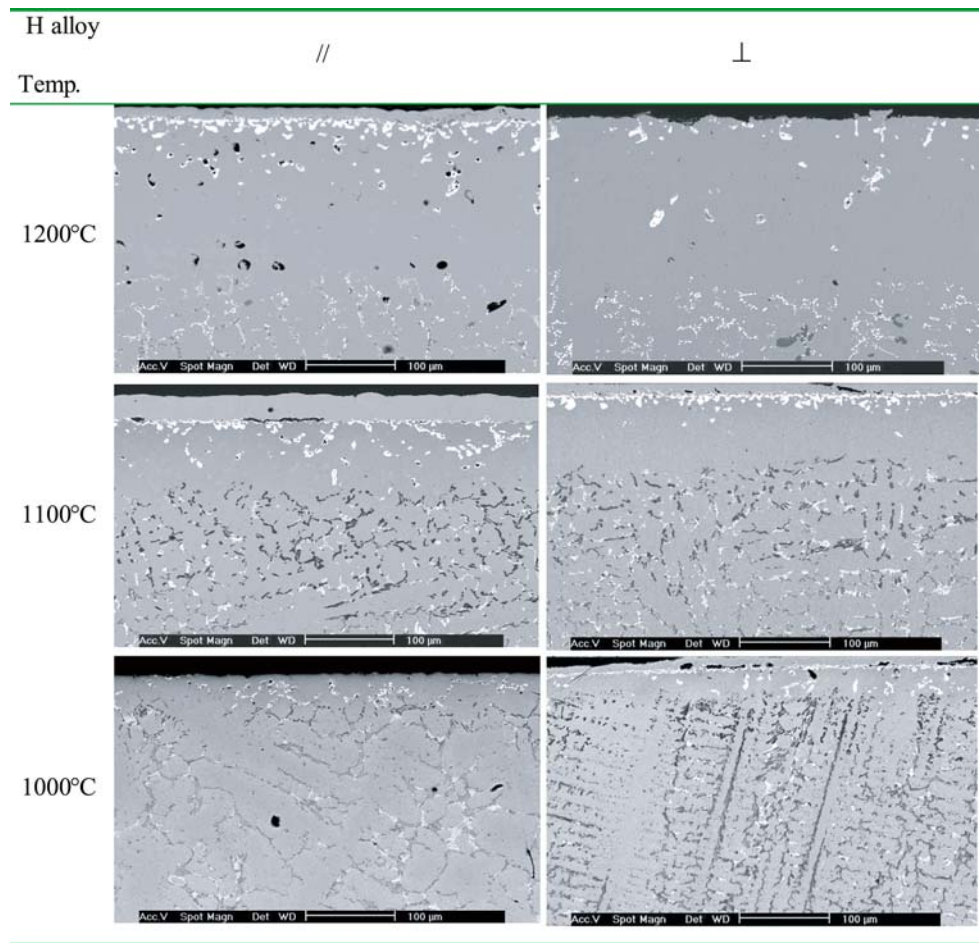
Table 6 Mean values of chromium gradients from the external surface

Alloy	Temperature (°C)					
	1,000		1,100		1,200	
	External	Internal	External	Internal	External	Internal
H alloy						
//	0.110%/μm over 24 μm	0.017%μm over 120 μm	0.038%/μm over 76 μm	0.008%/μ m over 203 μm	0.025%/μm over 260 μm	Too light
⊥	0.062%/μm over 36 μm	0.015%/μm over 101 μm	0.050%/μm over 66 μm	0.010%/μm over 174 μm	0.020%/μm over 270 μm	Too light
L alloy						
//	0.200%/μm over 20 μm	0.075%/μm over 50 μm	0.046%/μm over 95 μm	0.007%/μm over 150 μm	0.031%/μm over 275 μm	Too light
⊥	0.113%/μm over 40 μm	0.029%/μm over 70 μm	0.047%/μm over 90 μm	0.004%/μm over 220 μm	0.018%/μm over 265 μm	Too light

pointed out. Indeed, for 1,000 °C and for the two alloys, Cr gradients seems to be greater for the parallel orientation than for the perpendicular one, while such an order does not exist for 1,100 °C. For the L alloy at 1,200 °C, the Cr gradient for the parallel orientation is higher than for the perpendicular one again.

The tantalum profiles often present two successive gradients, especially in the case of L alloy. Like for chromium the gradients decrease and their depths increase when temperature increases. Gradients are generally more accentuated for H alloy than for L alloy, because of the higher Ta content of the first one. The total depletion is deeper for the L alloy than for H alloy. Except for the H alloy at 1,000 °C, the orientation does not sensibly influence the Ta gradients.

Table 7 Mean values of tantalum gradients from the external surface

Alloy	Temperature (°C)		
	1,000	1,100	1,200
H alloy			
//	0.054%/μm over 70 μm	0.038%/μm over 130 μm	0.028%/μm over 130 μm then 0.008%/μm over 80 μm
⊥	0.095%/μm over 40 μm	0.062%/μm over 45 μm then 0.014%/μm over 65 μm	0.010%/μm over 160 μm
L alloy			
//	0.049%/μm over 45 μm then 0.020%/μm over 40 μm	0.037%/μm over 35 μm then 0.013%/μm over 105 μm	0.011%/μm over 135 μm then 0.004%/μm over 195 μm
⊥	0.045%/μm over 40 μm	0.038%/μm over 40 μm then 0.009%/μm over 95 μm	0.009%/μm over 155 μm then 0.004%/μm over 165 μm
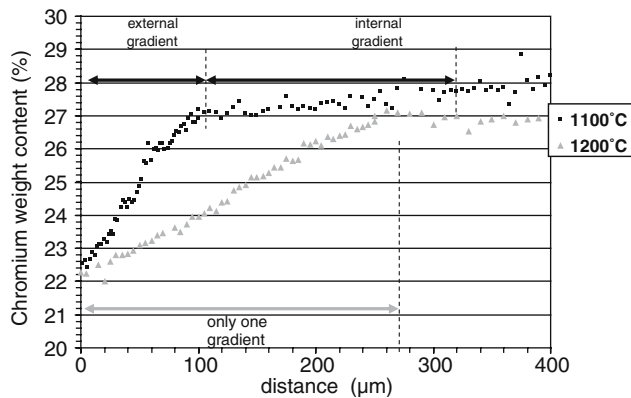
Fig. 9 Example of the two types of Cr profiles with two gradients or only one but deeper (here perpendicular-type L alloy after oxidation for 100 h at 1,100 °C and at 1,200 °C)

Discussion

Thermogravimetry results showed that the dendritic orientation can have an effect on the oxidation rate of these two nickel alloys. This was first seen for linear oxidation constants at all temperatures at the two highest temperatures. For the parabolic constant, a real difference appeared only for L alloy at 1,200 °C and for H alloy at 1,000 °C.

Concerning the transient linear oxidation, it is faster when dendrites are mainly perpendicular to the local external surface, than when they are parallel. The same observation can be made for the total mass gain obtained before the parabolic oxidation takes place. A perpendicular orientation is probably favorable to a more exposed position of emerging sub-surface carbides (i.e. their very oxidable Cr and Ta constitutive elements) to oxidation, in terms of density as well as of homogeneity. Then, transient oxidation and early

linear mass gain can be faster in this case than for the other orientation for which the presence of primary dendrites arms can act, here and there, as oriented barriers between interdendritic carbides and the external surface. The general nucleation of chromia (average number of nucleus per surface unit) could be also greater for the perpendicular orientation than for the parallel one, for the same reasons. The first lateral growth of the chromia can be accelerated until all these Cr_2O_3 crystals meet one another, leading to a faster mass gain during the transient oxidation for the perpendicular orientation than for the parallel one.

On the contrary, for the two cases where a real difference appeared, the Wagner's parabolic oxidation tends to be lower when dendrites are perpendicular to surface than when they are parallel. The same effect of the dendritic orientation on the values of the parabolic constant Kp was already found [2], but more marked, for a similar alloy (Ni–30Cr–0.7C–7.5Fe–7.5W) for which a sample with a surface mainly parallel to dendrites exhibited a higher Kp than a sample mainly perpendicular to dendrites. For the latter alloy it was found that $Kp_{//} \sim 3\, Kp_{\perp}$ at 1,000 °C, i.e. exactly what it was encountered here for the H alloy. It was also found that $Kp_{//} \sim 2\, Kp_{\perp}$ at 1,100 °C, i.e. exactly what it was found here for the L alloy but at 1,200 °C.

The faster oxidation for the parallel orientation could be explained by a less homogeneous chromia scale structure due to the dendrites orientation. Indeed grain boundaries are mainly parallel to surface and then they may induce an anisotropy (i.e. preferential orientations along the external surface) for the growth of external oxides. Thus one can think that the quality of external chromia scale is affected by this special texture. Then this chromia scale is less protective for the alloy, i.e. less favorable to a better resistance

against diffusion of the species involved by oxidation. Indeed, simple calculations from the depths and modulus values of Cr gradients allows to see that more chromium per surface unit left the bulk for the parallel orientation than for the perpendicular one for precisely the two cases where a real difference of Kp was seen: the mass of chromium lost by the H alloy after 100 h at 1,000 °C is 1.8 mg/cm^2 for the parallel-type sample and only 1.5 mg/cm^2 for the perpendicular-type sample (i.e. +20% for the // sample). For the L alloy after 100 h at 1,200 °C, these values are respectively 10.4 and 5.63 mg/cm^2 (i.e. +85% for //). These differences are sensibly higher than between the parallel-type sample and the perpendicular-type sample of H alloy at 1,100 °C (3.5 and 3.4 mg/cm^2 i.e. only +3% for //), H alloy at 1,200 °C (7.5 and 6.5 mg/cm^2 i.e. +15% for //), L alloy at 1,000 °C (1.9 and 2.2 mg/cm^2 i.e. +16% for ⊥) and L alloy at 1,100°C (3.4 and 3.3 mg/cm^2 i.e. +3% for //). Thus, despite of a greater difficulty due to diffusion paths not well oriented (difficulty revealed by the highest Cr gradients for the parallel orientation), more chromium often came on the oxidation front for the parallel orientation. Cr gradients were generally more marked for the L alloy for which the emerging interdendritic carbides are less dense and the primary dendrite arms coarser, than for H alloy.

On the contrary, no real differences were observed between the two orientations about the carbide-free zone depths and about the microstructure inner zone affected by oxidation, even for the two cases for which the parabolic constants were sensibly different between the two orientations.

Unfortunately, no analysis was possible on the chromia scale since the latter systematically quitted the alloy during cooling. Like for all chromia-forming alloys this phenomenon is possible since the average thermal expansion coefficient (about 7×10^{-6} °C^{-1}) is sensibly lower than our alloys' one (10×10^{-6} °C^{-1}), but the chromia exfoliation is probably worsen by the inner development of CrTaO$_4$ oxide just under chromia that does not allow a sufficiently good adhesion of chromia on the substrate. Previous oxidation tests performed on similar alloys also containing tantalum showed that slower cooling rates are not able to prevent this loss of the external oxide scale. One can also point out that the inner development of the CrTaO$_4$ has maybe also decreased the effect of dendritic orientation when the results of this study are compared to previous ones [2] obtained for a nickel alloy that did not contain tantalum. Such a role of tantalum can also be the reason why it was so difficult to obtain wholly parabolic mass gain curves (after the transient oxidation). Indeed, the lack of oxide adhesion due to the presence of CrTaO$_4$ between the alloy and the chromia layer can also make easier the exfoliation of chromia under the action of the oxide growth stresses. This is probably the origin of the too frequent jumps that affected the mass gain curves.

To finish one can notice that the greater differences about oxidation rates (linear and parabolic), and also sub-surface microstructure and concentration profiles, were generally seen between the two alloys: on the one hand lower transient and parabolic oxidation kinetics, and on the other hand deeper carbide-free zone, higher Cr gradients at 1,000 °C but deeper Ta depletions, were clearly found for the L alloy compared to the H alloy. These results are similar to those that were already found in previous studies concerning other carbides-strengthened cast alloys.

Conclusions

A dependence of the local parabolic oxidation rate on the dendrites orientation was found again for these tantalum-containing nickel alloys, but at only one of the three tested temperatures, a temperature which depends on the alloy. However, an effect of dendrites orientation was more frequently observed on the transient oxidation rate since the K_1 values were always higher for the perpendicular orientation than for the other one, especially at 1,200 °C. These results about Kp, confirmed by first simple Cr balance sheets, are similar to others obtained in previous works on other cast alloys, but they remain to be explained more precisely. Future works, on alloys which can more easily keep their external oxide during the isothermal stage as well as cooling down to room temperature, will certainly allow to notably better understand the role of dendrites orientation on the properties of the external chromia scale that can influence the oxidation behavior.

References

1. Kofstad P (1988) High temperature corrosion. Elsevier
2. Berthod P, Raude S, Renck AS, Rapin C, Podor R, Steinmetz P (2004) Mat Sci Forum 461–464:1117
3. Kurz W, Fisher DJ (1989) Fundamentals of solidification. Trans. Tech Publications
4. Lesoult G (1989) M59. Techniques De L'ingénieur
5. Lesoult G (1986) M58. Techniques De L'ingénieur

6. Berthod P (2005) Oxid Metals 64(3/4):235
7. Di Martino J (2002) Phd Thesis. Université De Nancy 1
8. Bradley EF (1998) Superalloys: a technical guide. ASM International
9. Sims CT, Hagel WC (1972) The superalloys. John Wiley & Sons
10. Berthod P, Michon S, Di Martino J, Mathieu S, Noel S, Podor R, Rapin C (2003) Calphad 27(3):279
11. Berthod P, Michon S, Mathieu S, Podor R, Rapin C, Steinmetz P (2004) Mat Sci Forum 461–464:1173
12. Berthod P, Véber C, Aranda L, Podor R, Rapin C (2005) Oxid Metals 63(1/2):57